

# **Conjugate heat transfer in a converging microchannel**

*A thesis submitted in partial fulfilment of the requirements  
For the degree of*

**Bachelor of Technology  
in  
Mechanical Engineering**

Submitted by:

**Amit Gupta**  
(Roll Number: 111ME0295)

Under the guidance of  
Prof. M.K. Moharana



Department of Mechanical Engineering  
National Institute of Technology Rourkela

June 2015



DEPARTMENT OF MECHANICAL ENGINEERING  
NATIONAL INSTITUTE OF TECHNOLOGY ROURKELA

## CERTIFICATE

This is to certify that the thesis entitled “**Conjugate heat transfer in a converging microchannel**” submitted to the National Institute of Technology, Rourkela by **AMIT GUPTA**, Roll Number: **111ME0295** in partial fulfilment of the requirements for the award of the degree of **Bachelor of Technology in Mechanical Engineering**, is a bona fide record of research work carried out by him under my supervision and guidance. The thesis, which is based on candidate’s own work, has not been submitted elsewhere for any degree/diploma.

Date: 03.06.2015

Prof. M.K. Moharana  
Department of Mechanical Engineering  
National Institute of Technology Rourkela  
Rourkela –769008

## **ACKNOWLEDGEMENT**

I would like to extend my heartfelt indebtedness to Prof. M.K. Moharana, Department of Mechanical Engineering, N.I.T Rourkela, for giving me this opportunity to work under him. Like a true mentor, he has supported and guided me in every step and also helped me to tackle every problem faced during the project. I find myself grateful to have him as my mentor. I would also like to thank Dr. S.S Mahapatra, H.O.D, Department of Mechanical Engineering, N.I.T Rourkela, for allowing me to work in lab for extended duration and granting access to departmental facilities.

In addition, I also wish to thanks Mr. Sangram (M. Tech) for his persistent support and guidance during the project.

**Amit Gupta**

**(111ME0295)**

## SELF-DECLARATION

I, Mr. Amit Gupta, Roll No. 111ME0295, a student of B. Tech (2011-15) from the Department of Mechanical Engineering, National Institute of Technology Rourkela do hereby declare that I have not adopted any kind of unfair and malicious means and carried out the research work ethically to the best of my knowledge. If adoption of any kind of unfair and malicious means is found in this thesis work at a later stage, then appropriate action can be taken against me including withdrawal of this thesis work and even withdrawal of the degree.

NIT Rourkela

03 June 2015

  
Amit Gupta

# CONTENTS

Abstract	vi
List of figures	vii
List of tables	viii
Nomenclature	ix
1 Introduction	1
1.1 Background	2
1.2 Introduction to heat transfer	2
2 Literature review	6
3 Problem statement	9
3.1 Introduction to CFD	10
3.2 Description of work	10
4 Results and discussion	15
4.1 Heat flux	16
4.2 Dimensionless wall and fluid temperatures	18
4.3 Nusselt number	19
4.4 Average Nusselt number	20
4.5 Comparison	20
5 Conclusion	23
References	25

## ABSTRACT

A numerical simulation is performed to comprehend the effects of axial back conduction in the solid substrate in a conjugate heat transfer having steady and laminar flow. A heat flux with constant magnitude is applied at the lower end of the substrate and the remaining surfaces were insulated. Working fluid used is water having slug velocity profile at the inlet of the channel. The thermal conductivity ratio ( $k_{sf}$ ) has been varied in a wide range of 0.33 to 702, thickness of the substrate has been changed for varying thickness ratio ( $\delta_{sf}$ ) of 1 to 4, keeping the width of substrate unchanged to quantify its effect on the axial back conduction and simultaneously, the Reynolds number is varied from 100 to 500. Simulations have been carried out with converging microchannel along with the straight microchannel with the dimension of inlet and outlet of the converging microchannel and the result is compared with converging microchannel and a systematic study was done to comprehend the effect of axial back conduction by varying all the parameters as mentioned above.

Keywords: converging microchannel, axial back conduction, conjugate heat transfer, Nusselt number.

## LIST OF FIGURES:

<b>Fig. No.</b>	<b>Title</b>	<b>Page no.</b>
1.1	Hydrodynamic entrance length in a circular tube	3
1.2	Thermal entrance length in a circular tube	4
1.3	Temperature variation of wall and fluid in case of constant heat flux	5
3.1	Schematic diagram representing a uniform cross-sectional microchannel with its cross-sectional area equivalent to that of inlet of converging microchannel	10
3.2	Schematic diagram representing a uniform cross-sectional microchannel with its cross sectional area equivalent to that of outlet of converging microchannel	11
3.3	Only the half of microchannel was involved for stimulation	12
3.4	Schematic diagram of converging microchannel	13
3.5	Axial variation of local Nusselt number with dimensionless axial distance for different grid sizes	14
4.1	Axial variation of dimensionless heat flux of converging microchannel	17
4.2	Axial variation of wall temperature and bulk fluid temperature of converging microchannel	18
4.3	Axial variation of local Nu in a converging microchannel	20
4.4	Average Nusselt number of the converging microchannel with the varying thickness ratio ( $\delta_{sf}$ ), conductivity ratio ( $k_{sf}$ ) and Re	20
4.5	Average Nusselt number of uniform and converging microchannels at $\delta_{sf} = 1$ , Re = 100 and $\delta_{sf} = 1$ , Re = 500	21
4.6	Axial variation of local Nu at varying $k_{sf}$ and Re for both converging as well as parallel wall microchannel	22

## **LIST OF TABLES**

<b>Table No.</b>	<b>Title</b>	<b>Page no.</b>
01	Different materials with their thermo-physical properties	14



## NOMENCLATURE

A	cross-sectional area ( $\text{m}^2$ )
CA	converging cross-sectional microchannel
$c_p$	specific heat ( $\text{J/kg K}$ )
d	circular duct diameter (m)
$D_h$	hydraulic diameter (mm)
$h_z$	local heat transfer coefficient ( $\text{W/m}^2 \text{ K}$ )
k	thermal conductivity ( $\text{W/m K}$ )
$k_{sf}$	wall to fluid conductivity ratio ( $k_s/k_f$ )
L	channel length (mm)
M	axial conduction number (-)
$\dot{m}$	mass flow rate ( $\text{kg/s}$ )
Nu	Nusselt number ( $h.D_h/k_f$ )
$q'$	average heat flux experienced at the substrate walls ( $\text{W/m}^2$ )
$q'_z$	average local heat flux at any location in axial direction ( $\text{W/m}^2$ )
r	radius (m)
Re	Reynolds number ( $\rho.u.D_h/\mu$ )
T	temperature (K)
UA	uniform cross-sectional microchannel
u	average fluid velocity ( $\text{m/s}^2$ )
$z^*$	non-dimensional axial distance along the channel length (-)

### Greek Symbols:

$\delta$	thickness (mm)
$\delta_{sf}$	thickness ratio of substrate to channel ( $\delta_s/\delta_f$ )
$\Delta T$	inlet and outlet temperature difference (K)
$\Theta$	non-dimensional temperature (-)
$\mu$	dynamic viscosity ( $\text{Pa.s}$ )
$\rho$	density ( $\text{kg/m}^3$ )

$\varphi$	non-dimensional heat flux (-)
$\omega$	width (mm)
$\omega_1$	inlet width (mm)
$\omega_2$	outlet width (mm)

**Subscripts:**

f	fluid
i	inlet condition, inner
m	mean
o	outlet condition, outer
s	solid
w	wall
z	axial length along the channel

# Chapter-1

## INTRODUCTION

## **1.1 Background**

The previous era has perceived swift progress in the development of microchannel based system and devices. Microchannels are the channel having characteristic dimension of few microns to hundred microns. The thickness of the substrate of microchannel is comparable to hydraulic diameter of the microchannel. The investigation of flow of fluid and transfer of heat in microchannels are becoming day by day very important because of its wide application in engineering problem such as microheat exchanger, microscale chemical reactors, biotechnology, industrial application and many more. Axial back conduction is the conduction in the solid substrate of channel due to the temperature gradient of the substrate in the direction opposite to the flow of fluid. Every channel is having axial back conduction but its effect on zero thickness substrate is very less and thus it can be ignored. During the design and analysis to calculate the heat transfer coefficient of the microchannel, the axial back conduction is ignored and this leads to errors in calculation and conclusion. Therefore, the conjugate heat transfer process (conduction as well as convection) cannot be ignored in microchannel. The conjugate heat transfer exists in all channels but other than microchannel, its effects are very less and thus it can be neglected. Now only pure convective heat transfer will not be considered to study the problem, due to axial back conduction it leads to conjugate heat transfer. The boundary conditions applied at a certain distance from the solid-fluid interface and this conjugate heat transfer in microchannel distorts the actual boundary condition imposed on the solid-fluid interface, reducing the overall heat transfer coefficient. The influence of axial back conduction gets magnified in microchannel systems and gives inaccurate heat transfer coefficient, if overlooked. The present study is concentrated on the numerical simulation of conjugate heat transfer and influence of axial back conduction on the converging microchannel.

## **1.2 Introduction to heat transfer**

Before proceeding further to comprehend the influence of axial back conduction in a conjugate heat transfer, one should have to understand the basic difference between the developing region and fully developed region for internal fluid flow in a duct.

A fluid with uniform velocity enters a circular duct. The fluid particles which are in contact with the wall come to complete stop because of no-slip condition and the layer adjacent to it slows down due to friction and the velocity at the middle portion of the pipe increases to

maintain the constant mass flow rate. Therefore, along the pipe a velocity gradient developed. The region in the flow up to which viscous effect is there due to fluid viscosity is called velocity boundary layer. As we move along the pipe in flow direction, the thickness of boundary layer increases and lastly it reaches the centre of pipe and the entire pipe filled. The region in the pipe from the inlet to the point where the velocity profile keep changing is called hydrodynamic entrance region and corresponding length from inlet to that point is called hydrodynamic entrance length. Since the velocity profile develops within entrance region, hence the flow is called hydrodynamic developing flow. The region after the entrance region where the velocity profile become constant is called hydrodynamic fully developed region. The profile of velocity in laminar flow in the developed region is parabolic whereas in turbulent flow it is slight flatter due to mixing along radial direction because of the eddy motion.

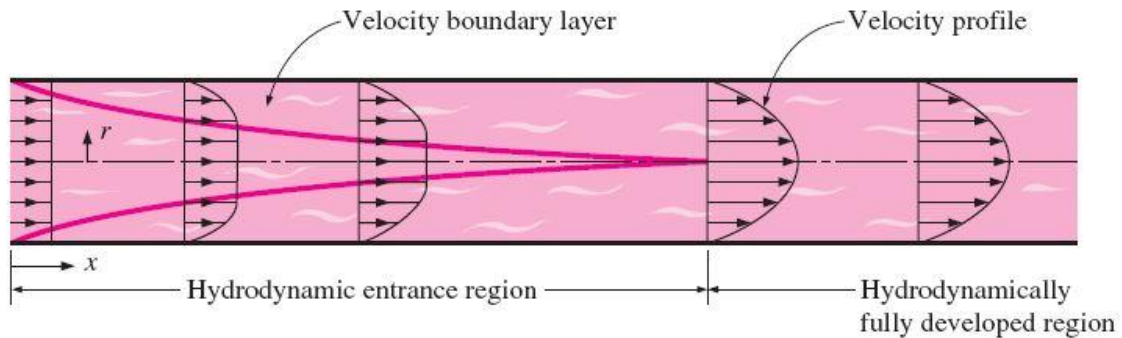


Figure 1.1: Hydrodynamic entrance length in a circular tube [1]

A fluid with uniform temperature enters a circular duct and a heat flux with constant magnitude is imposed on the circular duct, the heat is transferred through the circular duct by conduction and then it carried away by fluid through convection and the temperature of the wall and fluid keep on increasing along the circular duct in the flow direction. The region in the flow up to which the temperature profile keep changing is called thermal entrance region. Since the temperature profile develop within entrance region, hence the flow is called thermally developing flow. The region after the entrance region where the dimensionless profile become constant is called thermally developed region.

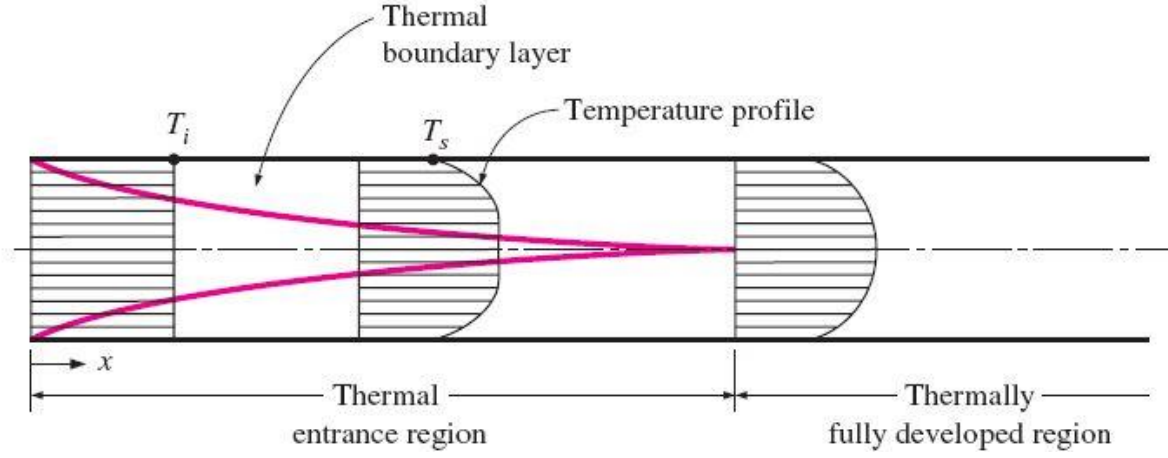


Figure 1.2: Thermal entrance length in a circular tube [1]

The mean temperature variation of wall and fluid in case of constant heat flux applied to the circular duct is shown below.

$$q' \cdot A_s = \dot{m} \cdot c_p \cdot (T_{f,o} - T_{f,i}) \quad (1.1)$$

Therefore the mean temperature of fluid at a position  $x$  becomes

$$T_x = T_i + \frac{q' \cdot A_s}{\dot{m} \cdot c_p} \quad (1.2)$$

The mean temperature of the fluid increases linearly along the direction of flow in a constant heat flux case. For the variation of wall temperature the equation is given below.

$$q' = h(T_s - T_m) \rightarrow T_s = T_m + \frac{q'}{h} \quad (1.3)$$

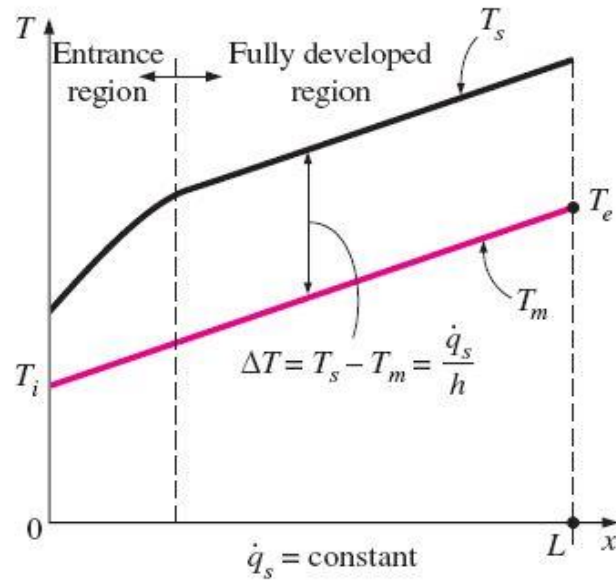


Figure 1.3: Temperature variation of wall and fluid in case of constant heat flux [1]

The variation of fluid and wall temperature for a circular duct in the direction of fluid flow subjected under constant heat flux is shown above. Within the developing region, the wall temperature vary exponentially in the direction of fluid flow and then it increases linearly.

# Chapter-2

## LITERATURE REVIEW



Bahnke and Howard [2] introduced the concept of “conduction parameter” while explaining the effect of longitudinal conduction of heat in the direction of flow for calculating the periodic flow heat exchanger effectiveness to measure axial conduction effect in the substrate in a single phase internal flow. It can be quantified as the ratio of transfer of heat along the solid substrate to the energy that is carried by fluid in the flow direction.

Axial conduction number (M) is introduced by Maranzana et al. [3] by considering the three non-dimensional parameter i.e. (a) Number of transfer units (b) Biot number (c) wall size ratio. Axial conduction number is defined as the ratio of heat flux due to conduction to the heat flux due to convection. Maranzana et al. [3] made an assumption that both the wall and fluid have the same difference in temperature between the inlet and outlet of the channel. The value of M is very low in the case of macrochannels because the thickness ratio ( $\delta_{sf}$ ) is low, high flow velocity and longer length of the channel and hence it can be assumed that the heat transfer due to conduction is only in one dimension but this situation deviates considerably in microchannel. Based on the above observation, they indicated that axial conduction effect can be neglected in the substrate if M less than  $10^{-2}$  while calculating heat transfer coefficient. Axial conduction number as well as conduction parameter are built by assuming that both the wall and fluid have the same difference in temperature between the inlet and outlet of the channel. To address this fault in defining the both parameter, Zhang et al. [4] introduced individually the effect of difference in temperature between the outlet and inlet of the solid wall and also the fluid. Li et al. [5] has given the revised conduction number. Numerical investigations were carried out by Zhang et al. [4] and the result indicated that condition ( $M < 10^{-2}$ ) as suggested by Maranzana et al. [3] is always not valid. They emphasized that substantial effect of axial back conduction in a circular duct was observed in spite of having the value of parameter (M) less than  $10^{-2}$ . Therefore, Maranzana et al. [3] criteria is not appropriate in the analysis of heat transfer in case of developing region of fluid flow in microchannel.

Numerous other criteria have been proposed by Lelea [6], Faghri and sparrow [7], Cotton and Jackson [8], Chiou [9], Petukhov [10] and many others. Hessel et al. [11] indicated that the axial conduction along the channel wall can be ignored if the parameter which is defined by Chiou [9] is not more than 0.005. Recently, Cole and Cetin [12] reported that the axial wall conduction is significant under the following cases (a) when the ratio of length to the height of microchannel is very minimal. (b) Small peclet number. (c) Large thickness of wall w.r.t

the height of channel. (d) High conductivity ratio ( $k_{sf}$ ) i.e ratio of solid conductivity to fluid. Moharana et al. [13] performed experimental and numerical investigation for a single phase hydrodynamically and thermally developing flow to comprehend the effect of axial back conduction in a rectangular minichannels array. It was found that at high value of axial conduction number (M), the situation leads to the case of conjugate heat transfer and value of Nusselt number obtained was smaller than the actual value and there was also variation of Nusselt number in axial direction. Moharana et al. [14] performed a numerical stimulation to comprehend the effect of channel aspect ratio on axial back conduction. The channel aspect ratio was varied from 0.45 to 4.0. At channel aspect ratio approximately two, the axial back conduction dominates which lead to conjugate heat transfer and minimum value of Nusselt number was obtained. Moharana et al. [15] carried out a numerical stimulation in a square microchannel by varying conductivity ratio ( $k_{sf}$ ), substrate thickness ratio ( $\delta_{sf}$ ) and Reynolds number. It was found that an optimum thermal conductivity ratio ( $k_{sf}$ ) exists for which the Nusselt number is maximized.

A numerical stimulation was performed by Moharana et al. [16] in a microtube at low temperature. Helium was used as a working fluid which enters at 100 K. The Reynolds number, thermal conductivity ratio ( $k_{sf}$ ) and radius to wall thickness ratio were varied. It was found that an optimum thermal conductivity ratio ( $k_{sf}$ ) exists for which the Nusselt number is maximized while the other parameters remain constant and further, the value of average Nusselt number decreases with increase in radius to wall thickness ratio and the value of average Nusselt number increases with the increase in the flow rate of helium.

Moharana et al. [17] performed a numerical simulation in a microtube which was partially heated. The Reynolds number, thermal conductivity ratio ( $k_{sf}$ ) and radius to wall thickness ratio were varied. The conductivity ratio ( $k_{sf}$ ) as well as thickness ratio play a prominent role. The average Nusselt number is higher for thinner wall but for very low conductivity ratio ( $k_{sf}$ ), thicker wall has high average Nusselt number value than the thinner one.

# Chapter – 3

## PROBLEM STATEMENT

### 3.1 INTRODUCTION TO CFD

CFD stands for Computational Fluid Dynamics. It is widely used for solving engineering problem which cannot be solved by analytically. The mass conservation, energy equations are non-linear partial differential equations which cannot be solved by analytically but an appropriate solution can be obtained by computer using CFD. Simulations can be performed using CFD in fluent software. The strategy used by CFD is that it uses discrete domain by choosing mesh or grid and replace the problem by continuous domain. The Navier-Stokes comparisons frame the premise of all CFD problems.

### 3.2 DESCRIPTION OF WORK

The main focus here is to find the effect of axial wall conduction in a conjugate heat transfer in a converging microchannel. The flow through the microchannel is single phase, steady state, laminar and incompressible. Heat flux with constant magnitude is imposed on the bottom wall of the solid substrate and the remaining parts are kept insulated. The working fluid used is water having slug velocity profile to the inlet of the channel and the flow rate of fluid is constant and thermo-physical properties are assumed to be constant. The thickness of the substrate has been changed, keeping the width constant, Reynolds number and conductivity ratio has been also varied.

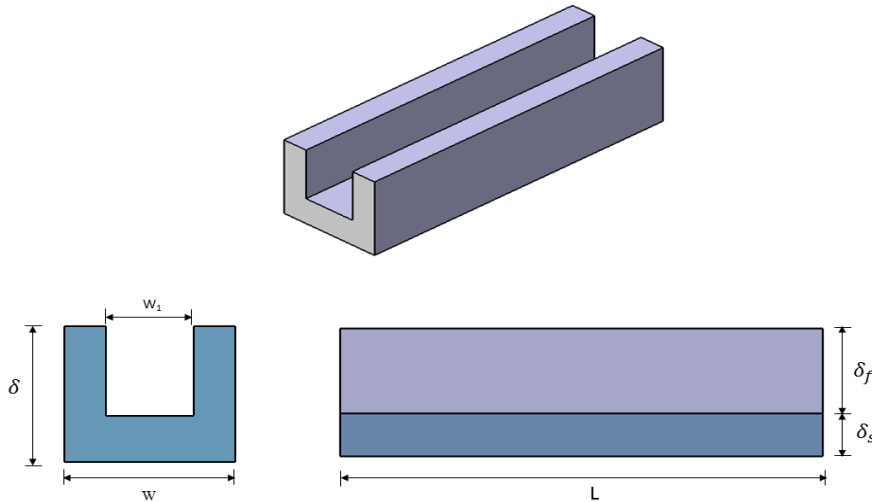


Figure 3.1: Schematic diagram representing a uniform cross-sectional microchannel with its cross-sectional area equivalent to that of inlet of converging microchannel

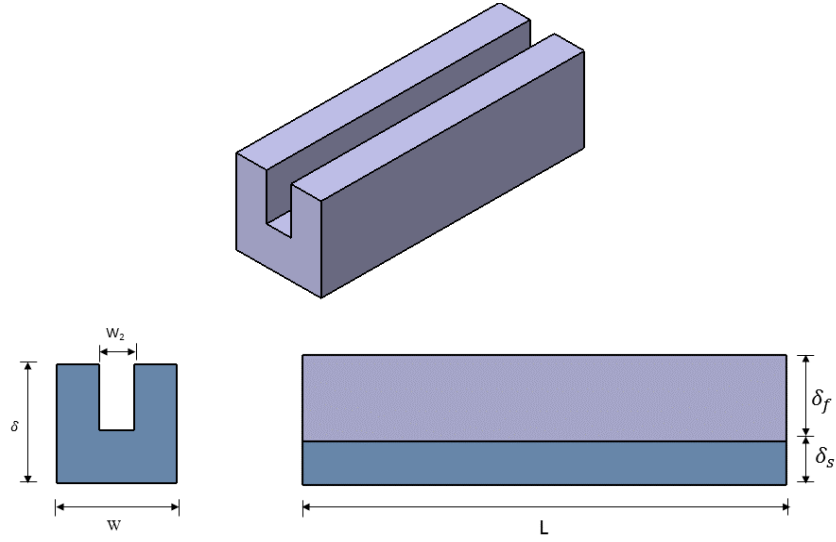


Figure 3.2: Schematic diagram representing a uniform cross-sectional microchannel with its cross-sectional area equivalent to that of outlet of converging microchannel

Width,  $W = 0.6$  mm,  $W_1 = 0.3$  mm,  $W_2 = 0.2$  mm, height  $\delta_f = 0.2$  mm, length  $L = 60$  mm

Hydraulic diameter is 0.24 mm. The portion  $(\delta_s + \delta_f)$  is changed, keeping the width constant.

For liquid region

$$\nabla \cdot \vec{u} = 0 \quad (3.1)$$

$$\vec{u} \cdot \nabla \vec{u} = -\frac{\nabla p}{\rho} + \frac{\mu}{\rho} \nabla^2 \vec{u} \quad (3.2)$$

$$\vec{u} \cdot \nabla T = \left( \frac{k}{\rho \cdot c_p} \right) \cdot \nabla^2 T \quad (3.3)$$

For solid region

$$\nabla^2 T = 0 \quad (3.4)$$

The following are the boundary conditions

$$\frac{\partial T}{\partial x} = 0; \text{ Plane Y-Z at } x = 0 \text{ and } x = 0.6 \text{ mm.} \quad (3.5a)$$

$$\frac{\partial T}{\partial y} = 0; \text{ Plane X-Z at } y = 0 \text{ and } y = 0.4 \text{ mm, } 0.6 \text{ mm and } 1 \text{ mm.} \quad (3.5b)$$

$$\frac{\partial T}{\partial z} = 0; \text{ Plane X-Y at } z = 0 \text{ and } z = 60 \text{ mm.} \quad (3.5c)$$

$u = 0$ ; no slip at all solid-fluid interfaces. (3.5d)

The axial conduction in the fluid is negligible because the Peclet numbers are large. The three dimensional numerical stimulation is carried out using the ANSYS-Fluent software to focus the effect of the conductivity ratio, substrate ratio and Reynolds number on local Nusselt number. Microchannel geometry is first generated in ANSYS 15 workbench and then it is properly meshed by using the grit size which was obtained after grit independence test. After that in set up window type of model is defined laminar, then material is selected as per the requirement and water is taken as working fluid. The energy equation was on and the value of heat flux is set. Atmospheric pressure is taken as operation condition and inlet temperature of fluid is taken as 300 °C. The second order upwind scheme was used to solve the energy and momentum equation. For better convergence, the value of residual is taken as  $10^{-6}$ . Then initialization is done and run for calculation.

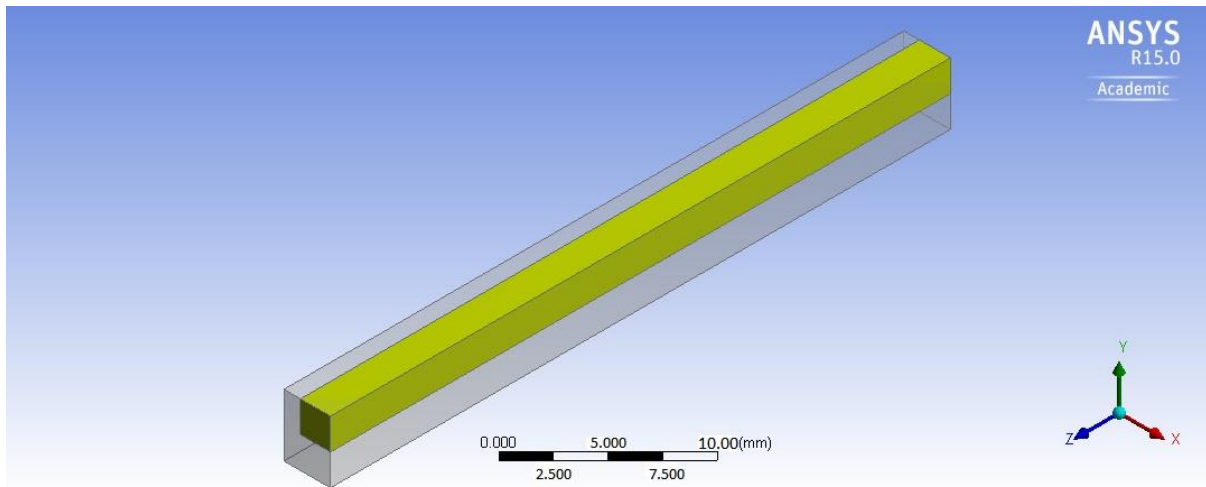


Figure 3.3: Only the half of microchannel was involved for stimulation

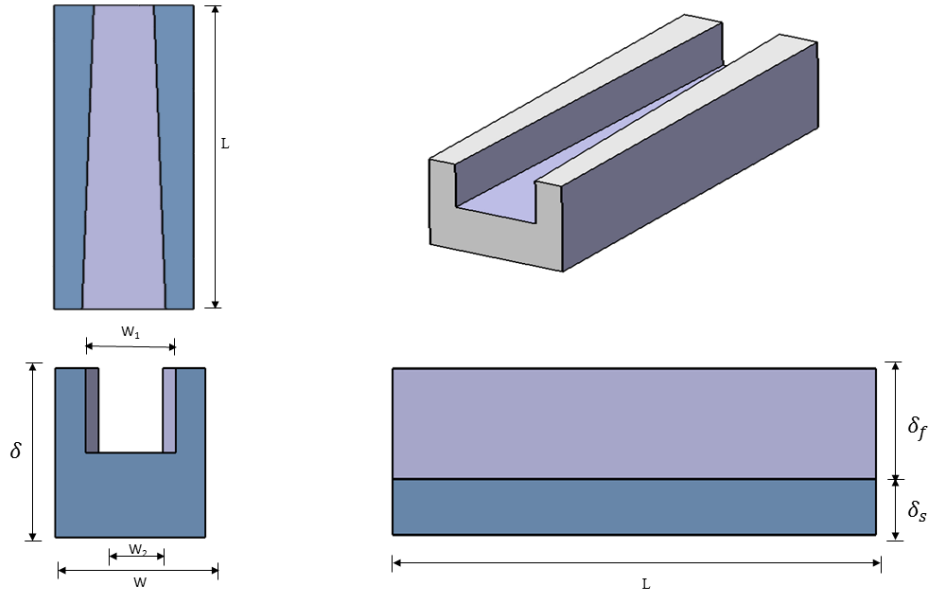


Figure 3.4: Schematic diagram of converging microchannel

In this study, the following non dimensional variables are used:

$$\phi = \frac{\overline{q'_z}}{q'}, \quad \delta_{sf} = \frac{\delta_s}{\delta_f}, \quad z^* = \frac{z}{\text{Re Pr } D_h}, \quad Nu_z = \frac{h_z D_h}{k_f} \quad (3.6)$$

$$\Theta = \frac{T - T_i}{T_o - T_i}, \quad \Theta_f = \frac{T_{f|z} - T_{fi}}{T_{fo} - T_{fi}}, \quad \Theta_w = \frac{T_{w|z} - T_{fi}}{T_{fo} - T_{fi}}$$

where  $T_i$  and  $T_o$  are temperatures of bulk fluid at inlet ( $z = 0$ ) and outlet ( $z = 60$ ).

$q'_z$  is the heat flux at location  $z^*$ .

Following formula is used to calculate the Nusselt number:-

$$Nu = \frac{q' \cdot D_h}{k \cdot (T_w - T_f)} \quad (3.7)$$

Average Nusselt number is calculated across the channel length as

$$\overline{Nu} = \int_0^l Nu_z dz \quad (3.8)$$

### Grid independence test

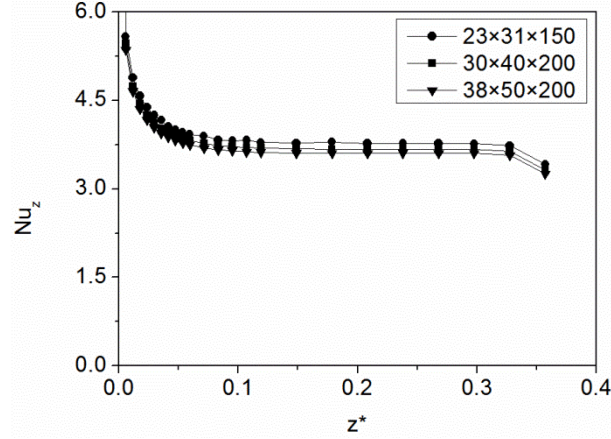


Figure 3.5: Axial variation of local Nusselt number with dimensionless axial distance for different grid sizes

For all geometries, grid independence tests were done. As an example, for a microchannel with substrate thickness ratio ( $\delta_{sf}$ ) one the local Nusselt number was obtained with three different grids of  $23 \times 31 \times 150$ ,  $30 \times 40 \times 200$ ,  $38 \times 50 \times 200$  for  $Re = 100$ . The local Nusselt number changes by around 1 % on an average as we move from  $23 \times 31 \times 150$  to  $30 \times 40 \times 200$  grid sizes and further the local Nusselt number changes by less than 1% from  $30 \times 40 \times 200$  to  $38 \times 50 \times 200$  grid sizes. Therefore the grid size of  $30 \times 40 \times 200$  was selected.

Different types of materials were used to carried out the three dimensional numerical stimulation. The list of materials are as follows:

Table 1: Different materials with their thermo-physical properties

Material	$\rho$ (kg/m <sup>3</sup> )	$C_p$ (J/kgK)	$k_s$ (W/mK)	$k_f$ (W/mK)	$k_{sf}$ ( $k_s/k_f$ )
Sulfur	2070	708	0.206	0.61032	0.338
Silicon dioxide	2220	745	1.38	0.61032	2.261
Bismuth	9780	122	7.86	0.61032	12.88
Nicrome	8400	420	12	0.61032	19.66
SS 316	8238	468	13.4	0.61032	21.96
Constantan	8920	384	23	0.61032	37.69
Chromium steel	7822	444	37.7	0.61032	61.77
Bronze	8780	355	54	0.61032	88.48
Zink	7140	389	116	0.61032	190.1
Alloy 195	2790	883	168	0.61032	275.3
Silver	10500	235	429	0.61032	702.9



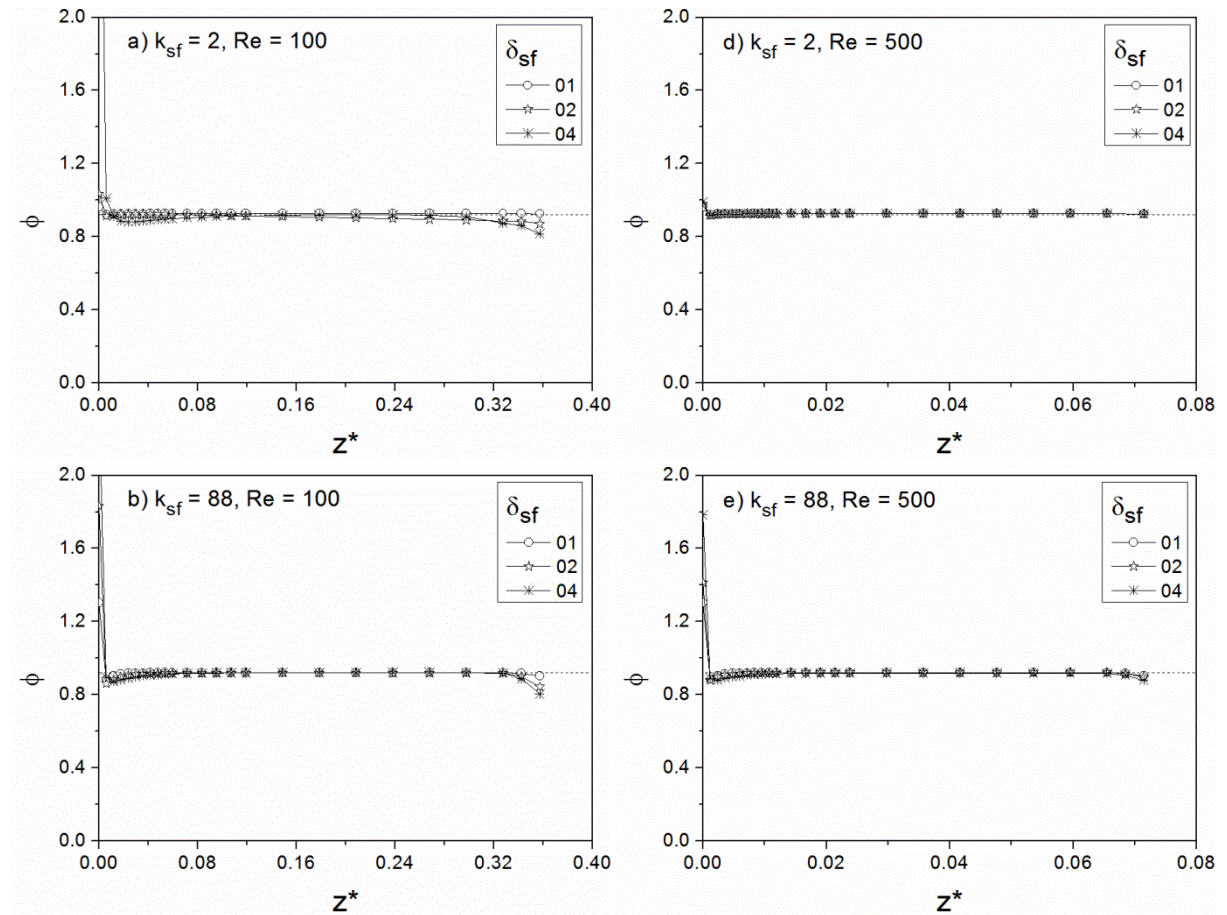
# Chapter – 4

## RESULT AND DISCUSSION

## RESULT AND DISCUSSION

A heat flux with constant magnitude is applied at the lower end of the substrate and the remaining surfaces were insulated. Thickness of the substrate has been changed from thickness ratio ( $\delta_{sf}$ ) of 1 to 4 and width remains unchanged to comprehend the influence of solid substrate thickness in heat transfer. Eleven materials have been changed varying thermal conductivity from 0.3 to 702 to comprehend the effects of thermal conductivity on heat transfer.

### 4.1 Heat Flux



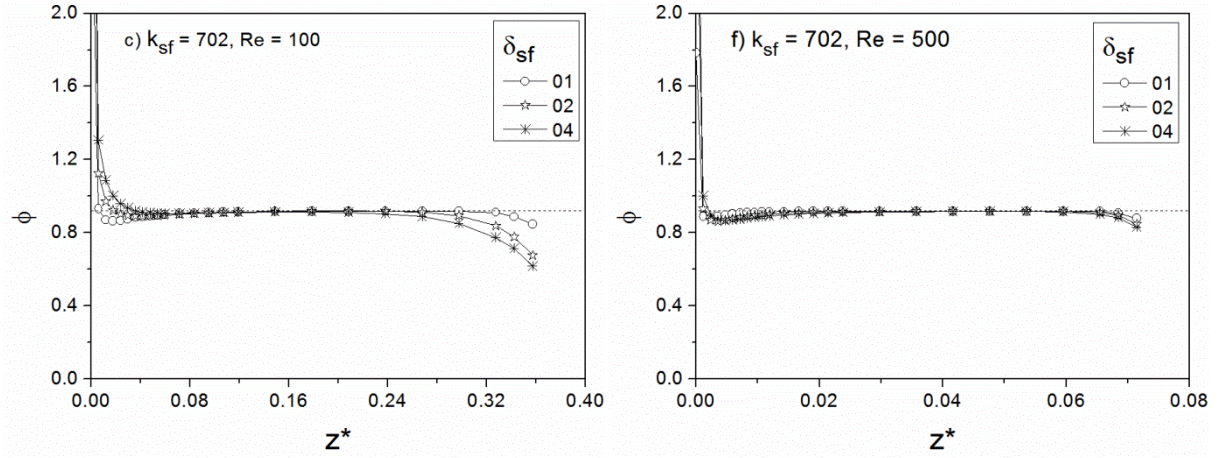


Figure 4.1: Axial variation of dimensionless heat flux of converging microchannel

The axial variation of heat flux has been shown in the above graph. At high thermal conductivity ratio ( $k_{sf}$ ), the value of heat flux value experienced at solid-fluid interface is not same as that of applied at the lower end of the substrate. At high conductivity ratio ( $k_{sf}$ ), the axial thermal resistance is lower which leads to axial back conduction and therefore, there is a distortion of the boundary condition at the conjugate walls and as the thickness ratio ( $\delta_{sf}$ ) increased, it further decreases the axial thermal resistance and more variations in the axial local heat flux occurs. But, the case is different at lower conductivity ratio. At lower conductivity ratio, the axial thermal resistance is very high and hence it become the case of zero wall thickness and the heat flux experienced at solid-fluid interface becomes same as that of applied at the lower end of substrate. At low thermal conductivity ratio ( $k_{sf}$ ), there is no effect of the variation in thickness in the value of heat flux experienced at solid-fluid interface. It has been observed that for a given  $k_{sf}$  and  $\delta_{sf}$  with increase in Reynolds number, the value of heat flux experienced at solid-fluid interface tends towards the ideal heat flux value given at the lower end of the substrate.



## 4.2 Dimensionless wall and fluid temperatures

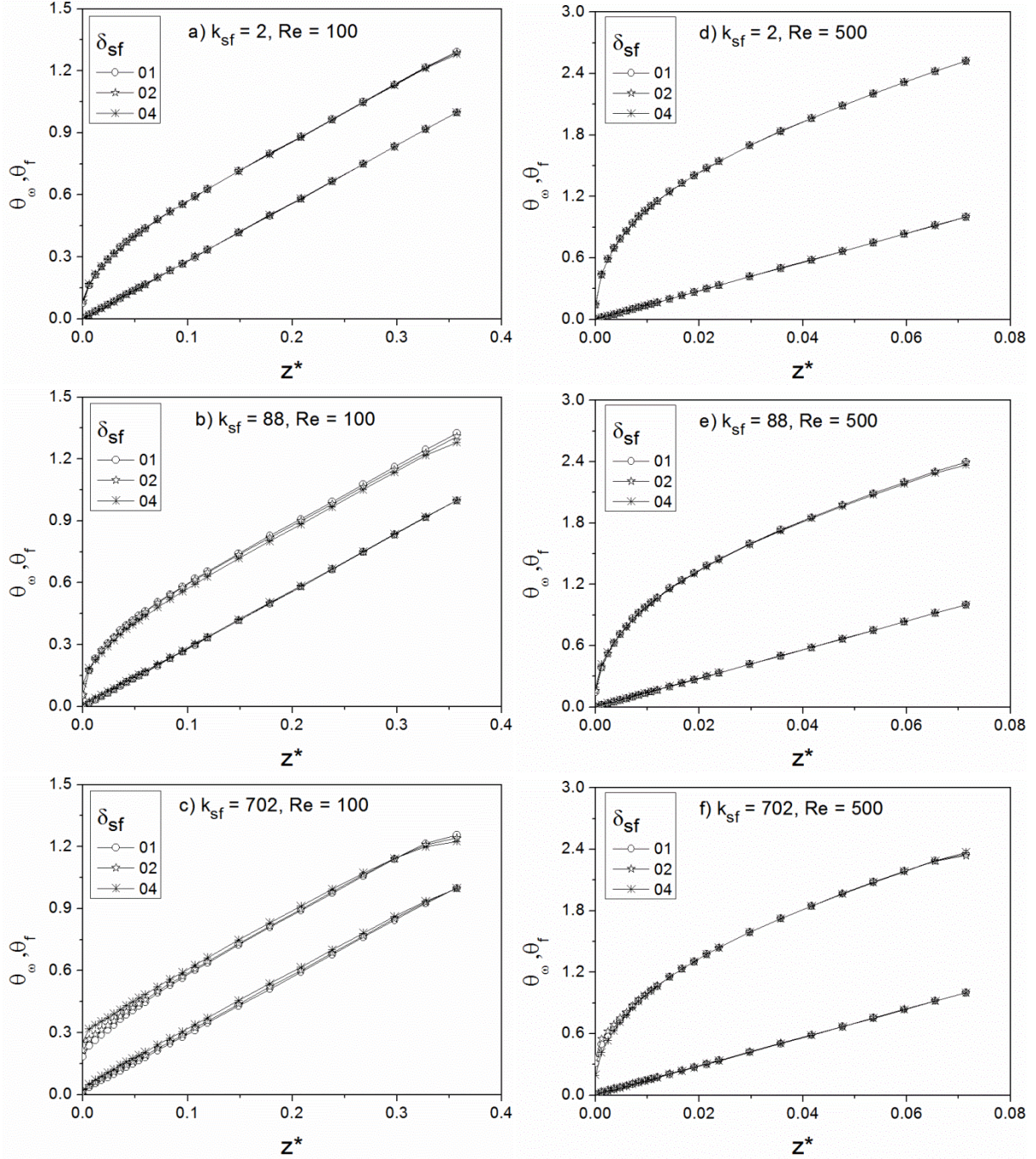
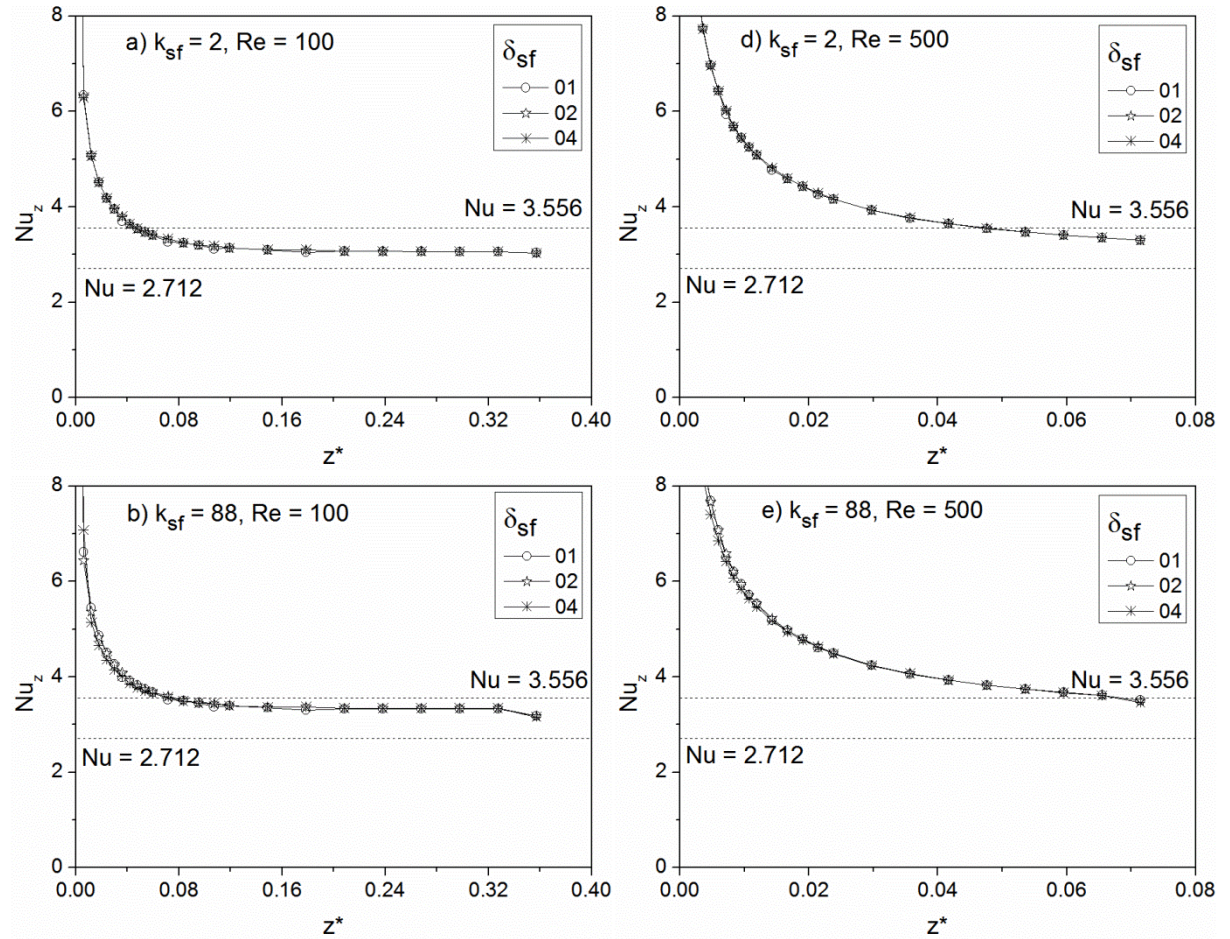


Figure 4.2: Axial variation of wall temperature and bulk fluid temperature of converging microchannel

The axial variation of the dimensionless wall and fluid temperature is shown in the above graph. At low conductivity ratio ( $k_{sf}$ ), the profile of fluid and wall temperature is similar to the case of zero wall thickness. Within the thermal entrance length i.e. developing region, the

difference between dimensionless wall and bulk fluid temperature increases and at fully developed region, the difference becomes constant. At low conductivity ratio, there is no variation in temperature profile with respect to thickness ratio ( $\delta_{sf}$ ). With the increase of conductivity ratio, the profile of dimensionless wall and fluid temperature deviated from the case of zero wall thickness. This deviation is due to axial back conduction because with increase of conductivity ratio, the axial thermal resistance decreases and the boundary condition at solid-fluid interface leads to pseudo-isothermal boundary condition instead of constant heat flux. At high conductivity ratio ( $k_{sf}$ ), the effect of thickness ratio ( $\delta_{sf}$ ) can be easily seen. The boundary condition gets more distorted with increase of thickness ratio ( $\delta_{sf}$ ).

### 4.3 Nusselt number





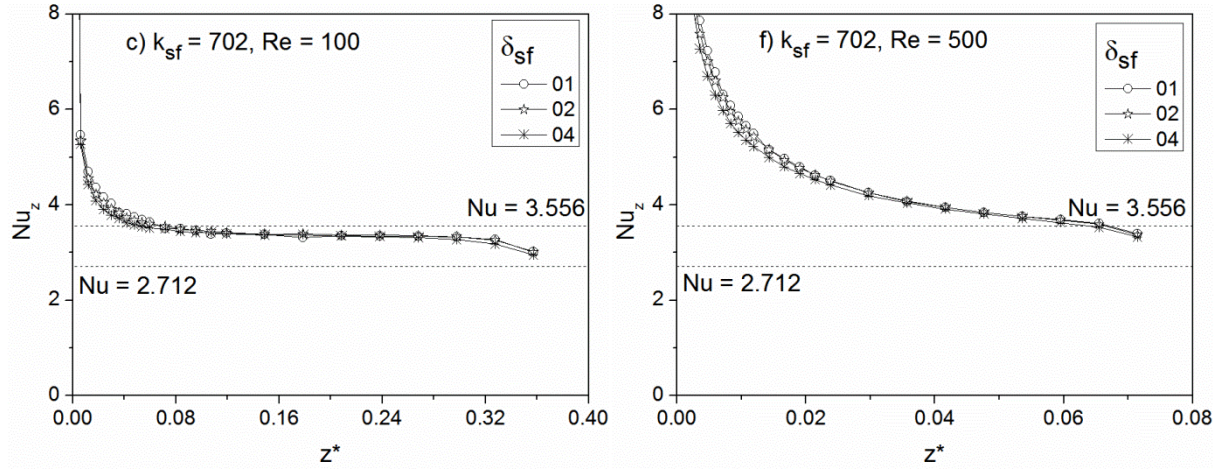


Figure 4.3: Axial variation of local Nu in a converging microchannel

The axial variation of local Nusselt number is shown in the above graph, the two asymptotes are drawn, one at the value of  $Nu = 3.556$  (square channel being heated from all the sides except the top side which is insulated) and other at the value of  $Nu = 2.712$  (square channel being heated from one side and all other sides being insulated). Both cases are of zero wall thickness. At  $k_{sf} = 88$ ,  $Nu$  converges less than 3.556 and no variation with  $\delta_{sf}$ . At high  $k_{sf}$ , it approaches to 3.009 with little variation with  $\delta_{sf}$ .

#### 4.4 Average Nusselt number

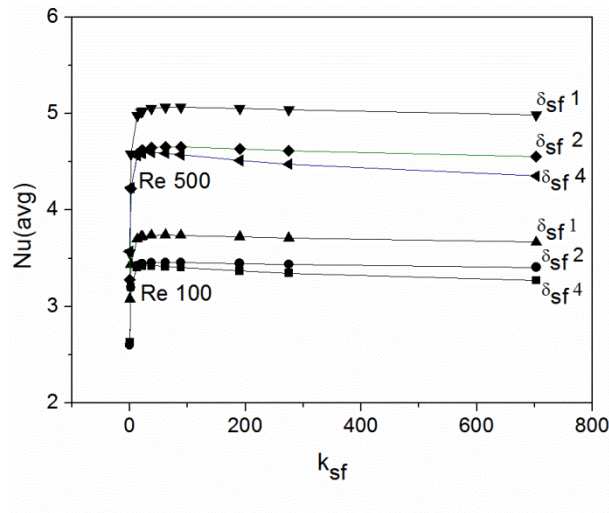


Figure 4.4: Average Nusselt number of the converging microchannel with the varying thickness ratio ( $\delta_{sf}$ ), conductivity ratio ( $k_{sf}$ ) and  $Re$

The variation of average Nusselt number with conductivity ratio has been shown in the above graph. The average Nusselt number is less at high thermal conductivity ratio ( $k_{sf}$ ). At very low thermal conductivity ratio ( $k_{sf}$ ), there is a change in spatial distribution of heat instead of

being transferred through bottom solid-fluid interface; it gets transferred through all the three conjugate walls of the channel to the fluid. Hence, there is an optimum  $k_{sf}$  for maximising the Nusselt number.

#### 4.5 Comparison

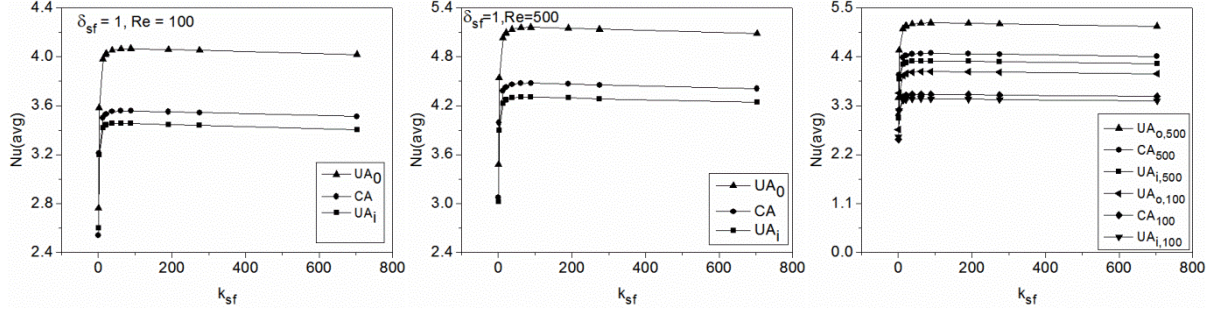


Figure 4.5: Average Nusselt number of uniform and converging microchannels at  $\delta_{sf} = 1$ ,  $Re = 100$  and  $\delta_{sf} = 1$ ,  $Re = 500$

The value of average Nusselt number obtained in converging microchannel is compared with the straight microchannel. Two straight microchannels have been taken with one dimension is of the inlet of converging microchannel and other is of the outlet of converging microchannel. The value of average Nusselt number is in between the value that is obtained from the straight microchannel. The straight microchannel with outlet dimension is having more value of average Nusselt number in comparison with the other two. For a laminar flow, the Nusselt number is directly proportional to square root of Reynolds number, and hence proportional to square root of velocity. For a given mass flow rate, the velocity is more in the microchannel with small cross-sectional area and therefore the straight microchannel with outlet dimension is having more value of average Nusselt number. Further, with increase in the value of Reynolds number from 100 to 500, the average Nusselt number increases in all of the three cases.

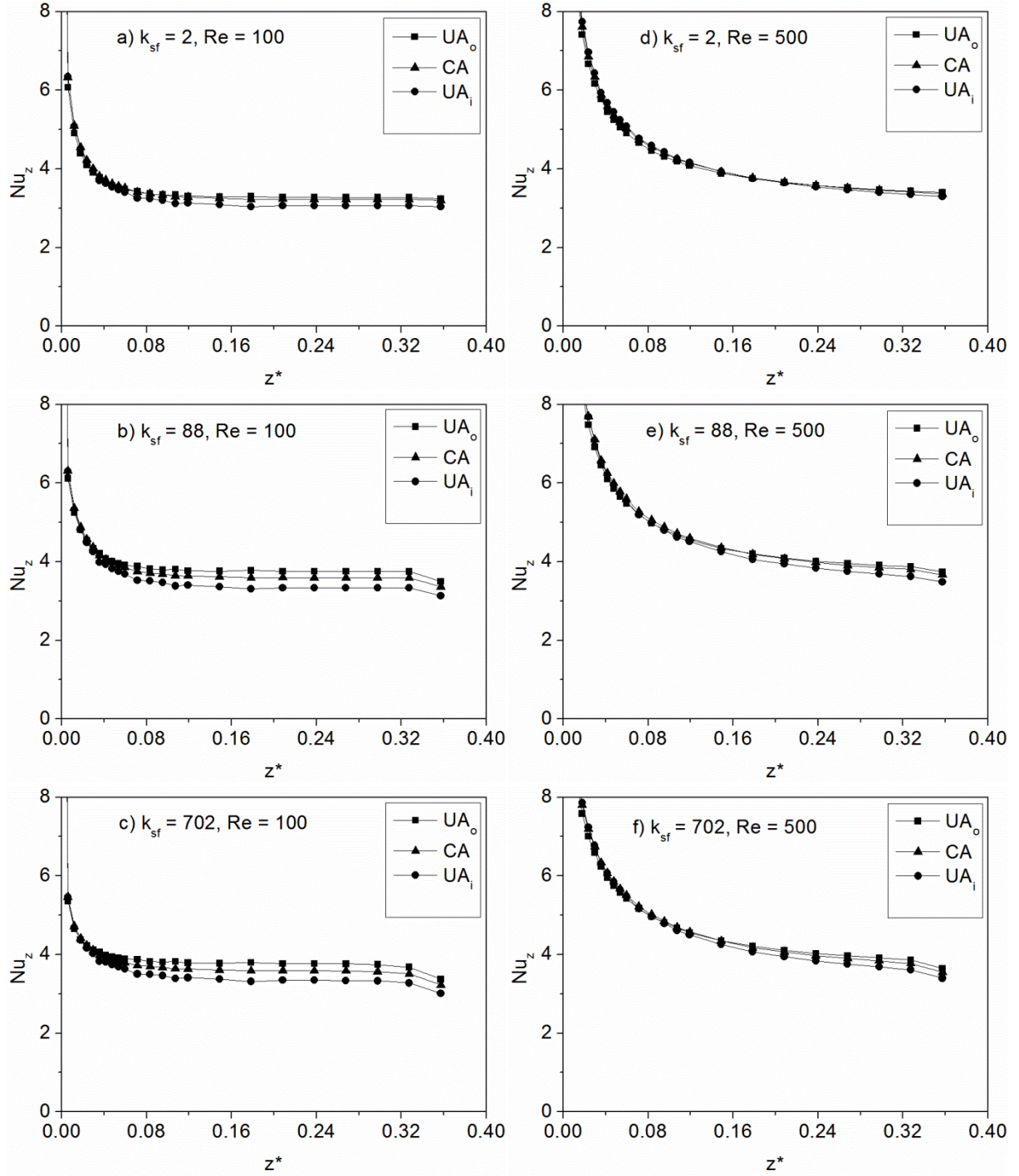


Figure 4.6: Axial variation of local Nu at varying  $k_{sf}$  and Re for both converging as well as parallel wall microchannel

The value of local Nusselt number obtained in converging microchannel is compared with the straight microchannel. The value of local Nusselt number is in between the value that is obtained from the straight microchannel for all the cases similarly to the value of average Nusselt number as mentioned above.



# **Chapter 5**

## **CONCLUSIONS**

## Conclusions

A numerical simulation is performed to comprehend the effects of axial back conduction in the solid substrate in a conjugate heat transfer having steady and laminar flow. A heat flux with constant magnitude is imposed on the lower end of the substrate and all the remaining surfaces are kept adiabatic. The thermal conductivity ratio ( $k_{sf}$ ) has been varied from a wide range of 0.33 to 702, thickness of the substrate has been changed from thickness ratio ( $\delta_{sf}$ ) of 1 to 4, keeping the width of substrate unchanged and the Reynolds number is varied from 100 to 500. From the above results, the followings have been concluded:

- For a given wall thickness ratio ( $\delta_{sf}$ ) and Re, the conductivity ratio ( $k_{sf}$ ) is the main parameter in deciding the effects of axial back conduction in case of the conjugate heat transfer problems.
- At high  $k_{sf}$ , the value of Nusselt number decreases because of axial back conduction as the axial thermal resistance decreases.
- At very low  $k_{sf}$ , the value of Nusselt number decreases as there is a distortion in the initial boundary condition imposed on solid-fluid interface.
- An optimum thermal conductivity ratio ( $k_{sf}$ ) exists for which Nusselt number is maximized.
- The similar results are obtained from uniform cross-sectional microchannel and the results for converging microchannel are in between the uniform cross-sectional microchannel.

## References

1. Cengel A. Y., and Ghajar A. J., 1998, "Heat and Mass Transfer," Tata McGraw Hill Education Private Limited, pp. 466-474.
2. Bahnke G. D., and Howard C. P., 1964, "The effect of longitudinal heat conduction on periodic-flow heat exchanger performance," *Journal of Engineering Power* 86(2), pp. 105–120.
3. Maranzana G., Perry I., and Maillet D., 2004 "Mini- and micro-channels: influence of axial conduction in the walls," *International Journal of Heat and Mass Transfer*, 47(17–18), pp. 3993–4004.
4. Zhang S. X., He Y. L., Lauriat G., and Tao W., 2010 "Numerical studies of simultaneously developing laminar flow and heat transfer in microtubes with thick wall and constant outside wall temperature," *International Journal of Heat and Mass Transfer*, 53(19–20), pp. 3977–3989.
5. Li Z., He Y. L., Tang G. H., and Tao W. Q., 2007, "Experimental and numerical studies of liquid flow and heat transfer in microtubes," *International Journal of Heat and Mass Transfer*, 50(17–18), pp. 3447–3460.
6. Lelea D., 2007, "The conjugate heat transfer of the partially heated microchannels," *Heat Mass Transfer*, 44(1), pp. 33–41.
7. Faghri M., and Sparrow E. M., 1980, "Simultaneous wall and fluid axial conduction in laminar pipe-flow heat transfer," *Journal of Heat Transfer*, 102(1), pp. 58–63.
8. Cotton M. A., and Jackson J. D., 1985 "The effect of heat conduction in a tube wall upon forced convection heat transfer in the thermal entry region," *Journal of Numerical Methods in Thermal Problems* T, Pineridge Press, Swansea, vol. Vol. IV, pp. 504–515.
9. Chiou J. P., Shah R.K.C., and McDonal C.C.F., 1980 "The advancement of compact heat exchanger theory considering the effects of longitudinal heat conduction and flow nonuniformity," *ASME-HTD Symposium on Compact Heat Exchangers*, vol. Vol. 10.
10. Petukhov B. S., 1967, "Heat transfer and drag of laminar flow of liquid in pipes," *Energiya*, Moscow.
11. Hessel V., Renken, A., Schouten J. C., and Yoshida J. eds., 2009, *Micro Process Engineering: A Comprehensive Handbook, Volume 1: Fundamentals, Operations and Catalysis*, Wiley-VCH, Weinheim, Germany.

12. Cole K. D., and Cetin B., 2011, "The effect of axial conduction on heat transfer in a liquid microchannel flow," *International Journal of Heat and Mass Transfer*, 54(11–12), pp. 2542–2549.
13. Moharana M. K., Agarwal G., and Khandekar S., 2011, "Axial conduction in single-phase simultaneously developing flow in a rectangular mini-channel array," *International Journal of Thermal Science*, 50(6), pp. 1001–1012.
14. Moharana M. K., and Khandekar S., 2013, "Effect of aspect ratio of rectangular microchannels on the axial back conduction in its solid substrate," *International Journal of Microscale and Nanoscale Thermal and Fluid Transport Phenomena*, vol. IV, no. 3-4, pp. 211-229.
15. Moharana M. K., Singh P. K., and Khandekar S., 2012, "Optimum Nusselt number for simultaneously developing internal flow under conjugate conditions in a square microchannel," *Journal of Heat Transfer*, (134) 071703, pp. 01-10.
16. Yadav A., Tiwari N., Moharana M. K., and Sarangi S. K., 2014, "Axial wall conduction in cryogenic fluid microtube," 5th International and 41st National Conference on Fluid Mechanics and Fluid Power (FMFP-2014) 12-14 December , IIT Kanpur, India.
17. Kumar M., and Moharana M. K., 2013, "Axial wall conduction in partially heated microtubes," in proceedings of 22th National and 11th International ISHMT-ASME Heat and Mass Transfer Conference, December 28-31, 2013, IIT Kharagpur, India.